SAND2007-0196C

High Efficiency DOEs at Large Diffraction Angles for Quantum Information and Computing Architectures

A. A. Cruz-Cabrera[a], S. A. Kemme[a], J. R. Wendt[a], D. Kielpinski[b], E. W. Streed[b], T. R. Carter[c], S. Samora[c]

ABSTRACT

We developed techniques to design higher efficiency diffractive optical elements (DOEs) with large numerical apertures (NA) for quantum computing and quantum information processing. Large NA optics encompass large solid angles and thus have high collection efficiencies. Qubits in ion trap architectures are commonly addressed and read by lasers[1]. Large-scale ion-trap quantum computing[2] will therefore require highly parallel optical interconnects. Qubit readout in these systems requires detecting fluorescence from the nearly isotropic radiation pattern of single ions, so efficient readout requires optical interconnects with high numerical aperture. Diffractive optical element fabrication is relatively mature and utilizes lithography to produce arrays compatible with large-scale ion-trap quantum computer architectures. The primary challenge of DOEs is the loss associated with diffraction efficiency. This is due to requirements for large deflection angles, which leads to extremely small feature sizes in the outer zone of the DOE. If the period of the diffractive is between λ (the free space wavelength) and 10λ, the element functions in the vector regime. DOEs in this regime, particularly between 1.5λ and 4λ, have significant coupling to unwanted diffractive orders, reducing the performance of the lens. Furthermore, the optimal depth of the zones with periods in the vector regime differs from the overall depth of the DOE. We will present results indicating the unique behaviors around the 1.5λ and 4λ periods and methods to improve the DOE performance.

Keywords: diffractive, numerical aperture, efficiency, blazed grating, ion-trap optics, optics for quantum information

1. INTRODUCTION

A conventional lens focuses by refracting light at the curved interface between materials of different refractive index. For small angles of deflection, a spherical surface is sufficient; however, at larger angles this introduces geometric aberrations. An aspherically shaped surface, Figure 1(a), can be engineered to correct these aberrations, with additional cost and complexity in fabrication with respect to conventional spherical lenses. In the wave picture of light, we can think of the lens as imparting a position-dependent phase with maximal constructive interference occurring at the focus.

Diffractive lenses can implement the same phase functions as refractive lenses. Figure 2 shows a cross-section of a diffractive lens and the resulting change in curvature of a wave front. The profile shows an eight-level stair-step phase lens whose periods decrease away from the center. Each period deflects and imparts a 2π phase delay with respect to the adjacent periods. If the phase jumps were unfolded, the diffractive lens profile would be stepped approximation of the equivalent refractive lens. This wrapping of the phase makes DOEs more wavelength sensitive than conventional optics. This is exploited in some commercial DOEs to correct chromatic aberrations. The quantum computing applications proposed here are monochromatic and are not susceptible to chromatic aberration.

---

[a]Sandia National Laboratories, Albuquerque, NM 87185-0603, USA
[b]Griffith University, Nathan 4111 Queensland, Australia
[c]L&M Technologies, Albuquerque, NM 87123, USA

Binary (two-level) DOEs have been demonstrated with a numerical aperture (NA) of 0.95 and 20% overall efficiency[3]. Our interest is in fabricating multilevel DOEs with higher efficiency to achieve diffraction-limited imaging[4] at high NAs.

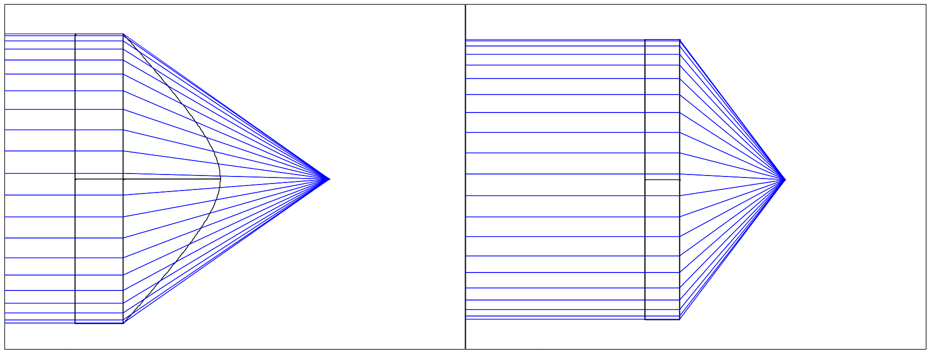

Figure 1 Depiction of an aspherical lens (a) with radius of curvature (ROC) of 1.066 mm, conic of -2.172 and a sagittal height of 2.676 mm for a numerical aperture (NA) of 0.8. Figure (b) depicts the equivalent diffractive lens for the same NA.

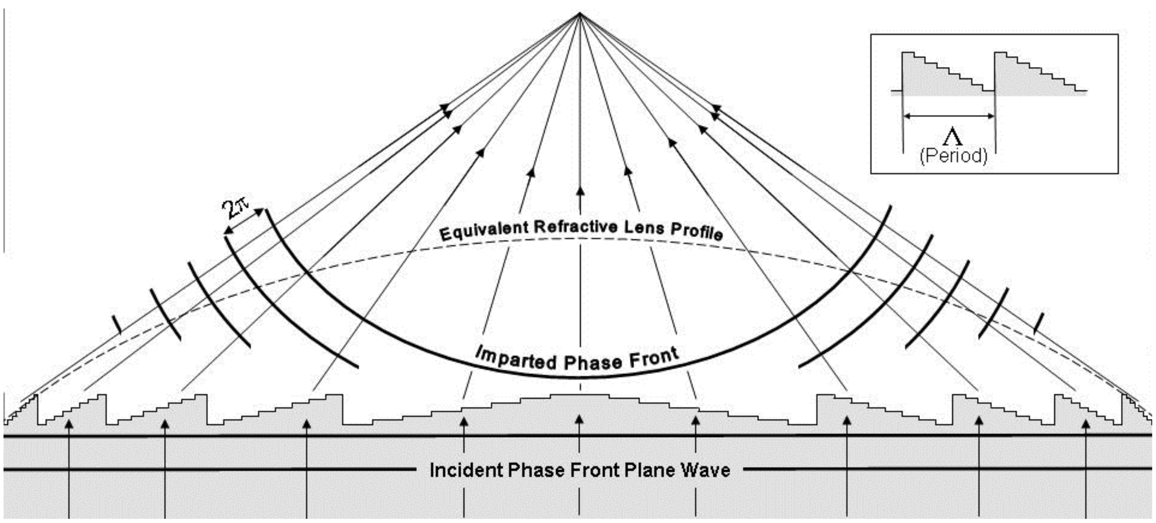

Figure 2 Representation of an 8-level diffractive lens cross section and the rays directions as a function of the lateral position of each period. The phase front is always perpendicular to the rays. In this case, the phase front is curved to focus the light. The dotted lines show the profile of an equivalent refractive lens.

The rays incident on a grating are diffracted with an angle, θ_{dm}, that is a function of the period, Λ, and the incident angle, θ_i, as seen in Equation 1:

$$\sin\theta_{dm} = \frac{m \cdot \lambda}{n_d \cdot \Lambda} + \frac{n_i \cdot \sin\theta_i}{n_d} \quad (1)$$

Where n_i is the refractive index of the incident medium, n_d is the refractive index of the diffracted medium, and m is the order of interest. For focusing applications, m is 1. Figure 3 indicates the existence of other orders, but the intent here is to suppress them. Equation (1) shows that, as the period gets smaller, θ_{dm} gets larger, explaining why the periods decrease away the focusing lens center.

Figure 4 shows a scanning electron micrograph (SEM) of diffractive lenses that focus and divert a laser beam in an optical interconnected microsystem at Sandia National Laboratories[a].

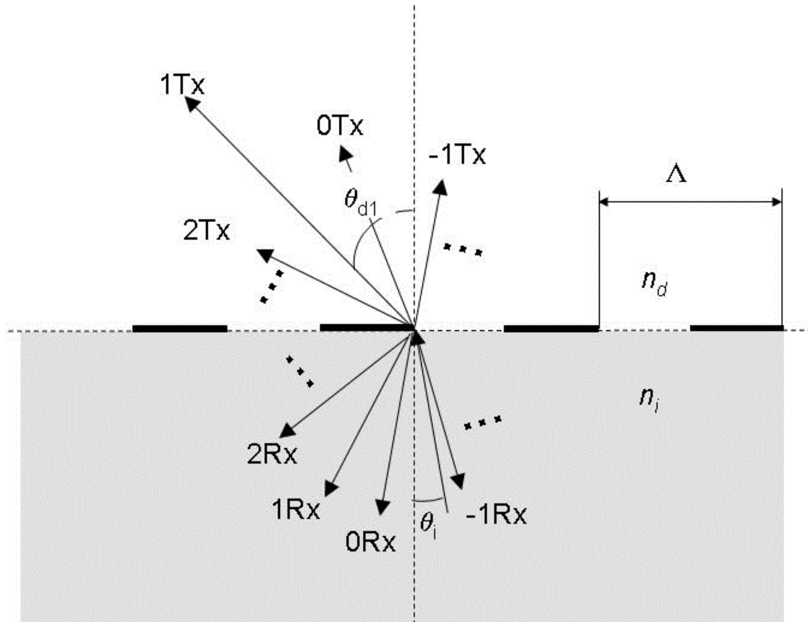

Figure 3 Depiction of the output angles as a function of grating period, refractive indices, and order number. The diagram shows some of the transmitted and reflected orders.

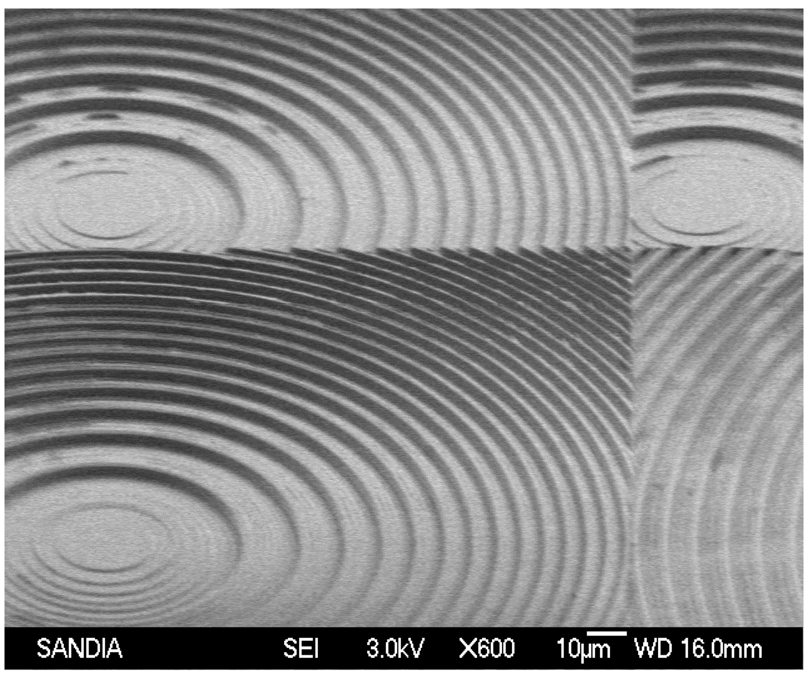

Figure 4 Scanning electron micrograph (SEM) of a portion of the optical interconnect array in fused silica, fabricated at Sandia National Laboratories[a]. The lenses are used at 1.55μm and have NAs that range from 0.17 to 0.5.

2. EFFICIENCY CALCULATION

To quantify the DOE efficiency we use a rigorous coupled wave analysis (RCWA)[5] code. RCWA strictly solves for the magnitude and phase of the output electromagnetic field.

The first order transmitted efficiency graphs versus grating period and total grating depth are shown in Figure 5. The calculation uses a fused silica substrate at a wavelength of 0.37μm and assumes an input polarization of 45-degrees at normal incidence. The 45-degree polarization is selected because the lens is radially symmetric, and the total effects of using the correct polarization for each rotation angles will average to a calculation with a 45-degree polarization.

Figure 5(a) quantifies a four-level grating and Figure 5(b) an eight-level grating. The period range of analysis is from 0 to 3.7μm (10 λ), and the depth range is from 0 to 1.2μm. The graphs show an area of high efficiency for periods between 2 and 3.7μm and for depth range of 0.4 to 0.8μm. The efficiency drops pronouncedly as the period is reduced from 3.7μm to 0.7μm. For a period between 0.37 and 0.6μm the efficiency peaks again. For periods smaller, than 0.37μm the component is subwavelength, where the 1^{st} order no longer propagates and the 0^{th} order contains all the energy.

The black lines in Figure 5(a) and Figure 5(b) denote the efficiencies at constant depths for four- and eight-level gratings. Figure 6 shows these efficiencies from $\Lambda = 0$ to 10λ for four- and eight-level gratings using RCWA.

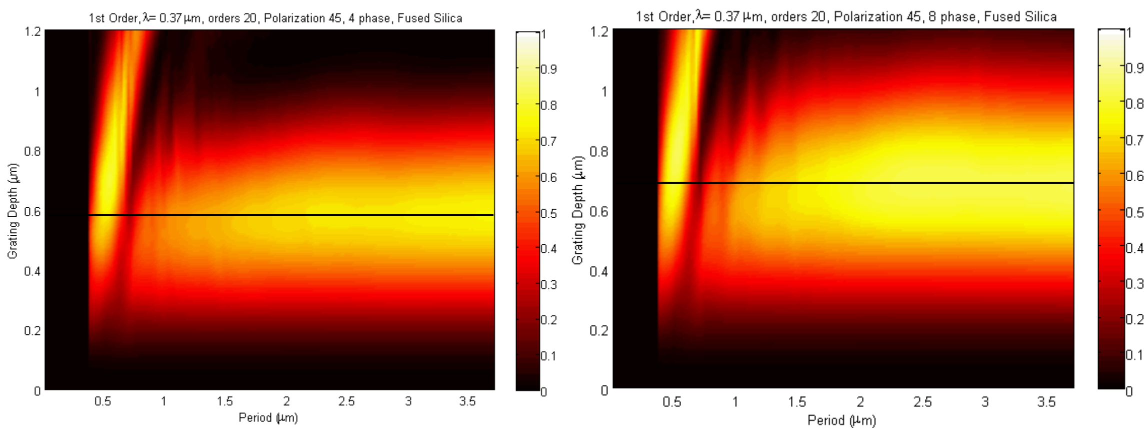

(a) (b)

Figure 5 Rigorous coupled wave analysis (RCWA) simulations for first transmitted order of a four- (a) and eight- (b) phase level grating in fused silica. The simulation uses a wavelength of 0.37μm, a 45-degree polarization, and normal incidence. The graph depicts the response to changes in diffractive period versus total depth. The horizontal black line indicates the efficiency response for a typical DOE lens whose depth is determined by the scalar equation.

RCWA shows this is a unique regime with high efficiencies for the +1 transmitted order, Figure 6. At a period of 0.5μm, the +1 transmitted order is dominant while other orders are suppressed. As the period increases toward 0.7μm, the +1 order decreases to less than 30%. Here the four-level grating has a higher efficiency than the eight-level device for periods no larger than 1μm.

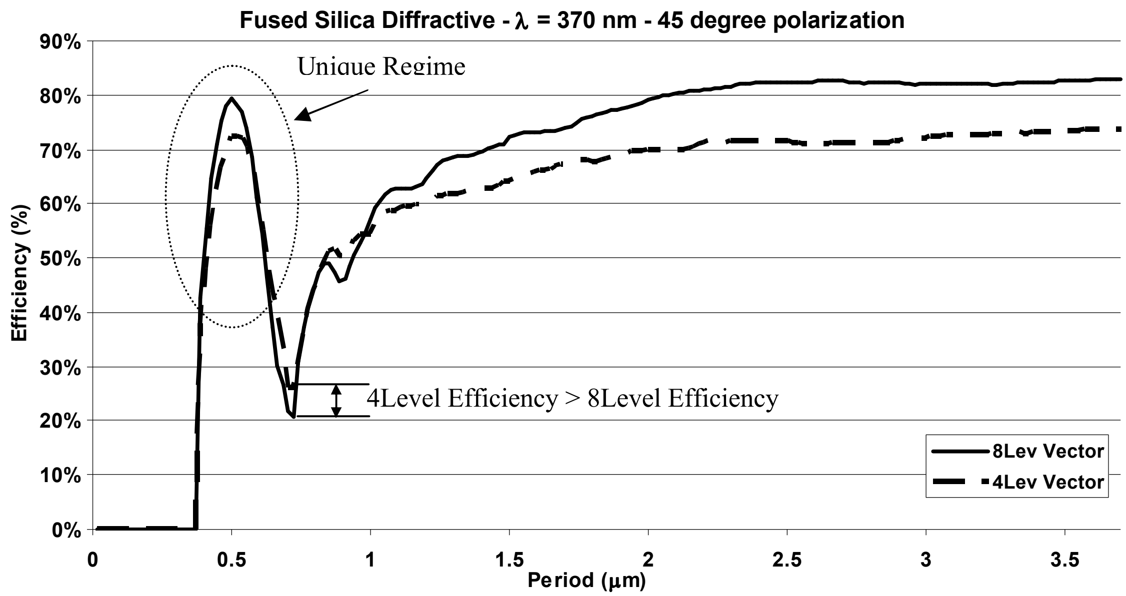

Figure 6 RCWA simulations of the first transmitted order for four- and eight-level gratings as function of the period for a fixed depth. Notice the larger efficiency for the four-level compared to the eight-level grating at the dip in efficiency around the period of 0.7μm for RCWA. The simulation uses a wavelength of 0.37μm, a 45-degree polarization, and normal incidence in fused silica.

3. OVERALL LENS EFFICIENCY

To calculate the actual efficiency of a full DOE lens, we sample the periods at well-defined annular intervals and calculate the grating efficiency for the dominant period at that interval using RCWA. The percentage of energy diffracted is calculated by techniques developed by Swanson[6] and added to the other intervals. This approach allows the calculation of efficiencies for any beam size and distribution, and for non-radially symmetrical lenses. For our calculations, we assumed that the incident light would have a Gaussian irradiance distribution to model light from an optical fiber or laser.

Several sets of diffractive lenses were fabricated for wavelengths of 0.85μm and 1.55μm. The lenses are eight-level and some are a mixture of eight- and four-level gratings. Figure 7 depicts their measured efficiencies and for some, their predicted values as a function of the lens NA. The two 0.85μm lenses were fabricated and tested for different output NA, with both lenses working on-axis. One of the lenses has the smallest gratings optimized, "8Lev-Opti-Measured-0.85μm," which improves its efficiency when the output NA is larger than 0.65. The efficiencies for the three DOE lenses for the 1.55μm application were predicted and measured. The graph indicates that the fabricated devices were 2 to 6 percentage points below the predicted efficiencies. The highest-efficiency DOE works on axis and its NA is around 0.17. The other two DOEs are used off-axis and impart 21 and 15 degrees to a focusing beam. These two DOEs are subsections of equivalent lenses with NAs of 0.5 and 0.38, respectively. We replaced the eight-level gratings with four-level gratings in sections of these lenses.

Figure 8 shows the estimated efficiency using RCWA for a lens designed with an NA of 0.8 in fused silica for a wavelength of 0.37μm. The figure shows the efficiency of the lens for different input beam sizes and consequently different NAs. By assuming that the beams hit the center of the lens, it is possible to see that as the beam get smaller, the requirement for large diffractive angles reduces, and the overall efficiency increases. In addition, it indicates that an eight-level DOE, compared with a four-level DOE, will be 10 to 12 percentage points more efficient with a smaller NA requirements, but the difference will reduce to less than 5 percentage points when the NA requirements exceed 0.7.

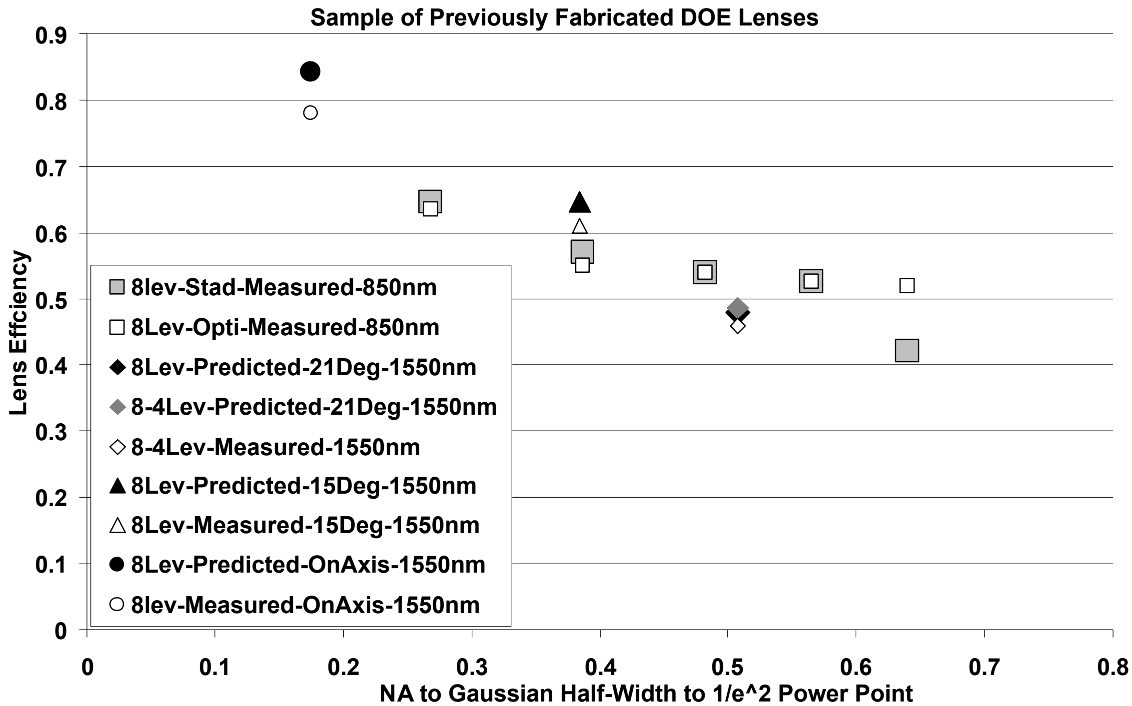

Figure 7 Simulated and fabricated eight-level DOEs. The graph shows the efficiency response to the beam $1/e^2$ radius. The lenses not only focus to a spot but also impart an angle to the beam.

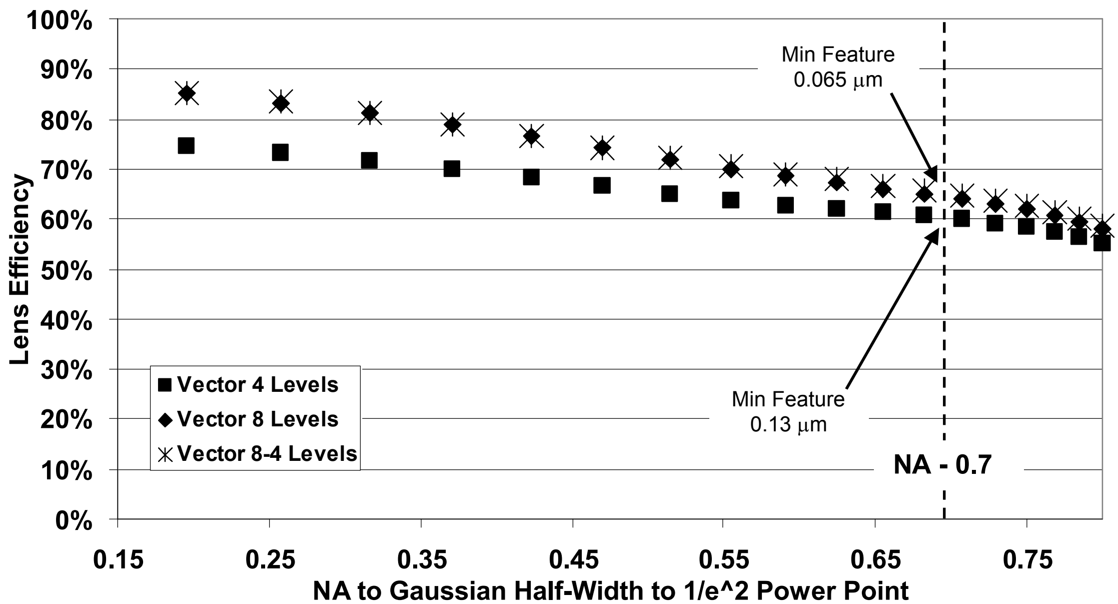

Figure 8 RCWA predicted efficiencies for lenses with different numerical apertures (NA) and number of levels. The model assumes a normal-incidence collimated beam with a wavelength of 0.37μm and 45-linear polarization.

Figure 8 shows that for higher efficiency requirements, it is possible to replace eight-level gratings with four-level gratings around the periods where the first order efficiency is lower than 50%. In this case, the four-level has a slightly higher efficiency than the eight-level, see Figure 6, and it is easier to fabricate.

4. EFFICIENCY IMPROVEMENT TECHNIQUES

If the grating depth can be optimized for each period, the grating with a period close to 0.7μm would have a depth of 1 to 1.2μm and have a first order efficiency close to 70%, see Figure 5(a) and Figure 5(b). The difficulty with a variable grating depth approach is that the number of fabrications steps increases by multiples of the number of zones with optimized depths. A standard eight-level grating has 28 fabrication steps, and optimizing the depth for three zones will increase the number of steps to more than 84.

Another approach to improving the efficiency of DOEs is to change the feature sizes, Figure 9(a), to an unconventional set of dimensions, Figure 9(b). Notice that Figure 9(a) shows the extreme case where the diffractive efficiency is minimal, 27%, and changing the features of the grating more than doubles it to 63%.

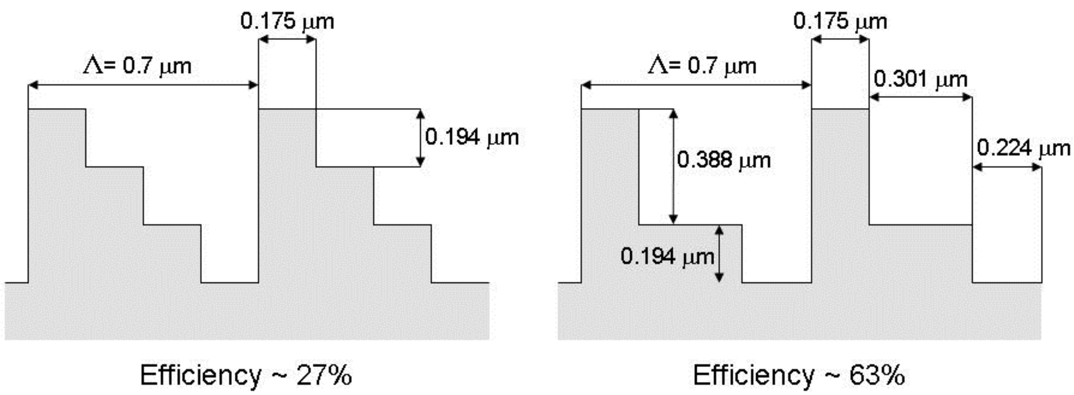

(a) (b)

Figure 9 Simulation results for the first transmitted order of a standard four-level (a) grating with a period of 0.7μm. The change of the feature sizes of the stair step (b) improves the first order efficiency of the diffractive at those small periods.

5. PROXIMITY CONSIDERATIONS

Integration of optics with ion-trap devices is challenging because the electric field configurations used to trap ions are easily distorted by nearby materials, whether insulating or conducting. Charging of insulating surfaces presents especially severe problems, as the random nature of the charging cannot be compensated for the trap design. Optics are usually kept several millimeters from the trap electrodes to minimize these effects, so that high numerical apertures can only be achieved by macroscopic optics. One way to alleviate surface charging is by grounding the lenses. This can be achieved by depositing a thin film of indium tin oxide (ITO), refractive index at 0.37μm of $\tilde{n}$ = 2.1619+0.0319i (extrapolated from Craciun et al.[7]), on top of the diffractive lens. ITO is conductive, but still relatively transparent to the working wavelengths.

The problem with thick films is that they may not be conformal so that the original shape of the grating is smoothed out. This variation in the geometry of the gratings may degrade the efficiency of the lens.

We looked at a four-level grating and modeled the element for periods between 0 and 3.7μm at a wavelength of 0.37μm with normal incidence and a 45° polarization. The DOE is made in fused silica. We modeled a bare device, one coated with 100Å of ITO, and one coated with 200Å of ITO. For the coated devices, we assumed two extreme cases: One where the coating is completely conformal and another one where there is no coating on the vertical walls, just ITO caps, see Figure 10. Not having an ITO coating on the vertical wall is undesirable for the electrical performance of this application, but it is a real possibility. Nevertheless, we estimate that the coating in the vertical walls may vary from 25% to 50% of the target thickness.

As expected, the modeling indicates that the bare DOE is the most optically efficient of the five options, see Figure 10. The DOE with 100Å of ITO drops the optical performance by 4%, and the one coated with 200Å by 12%. There is a minor difference in efficiency between conformal coating and caps for large periods. As the periods get smaller, the conformal devices have 2% to 5% losses. This makes sense given that the coating in the vertical wall is now a significant percentage of the feature size of the grating and is reducing the feature size at the bottom of the stair step. Most of the losses are related to the absorptive nature of the ITO.

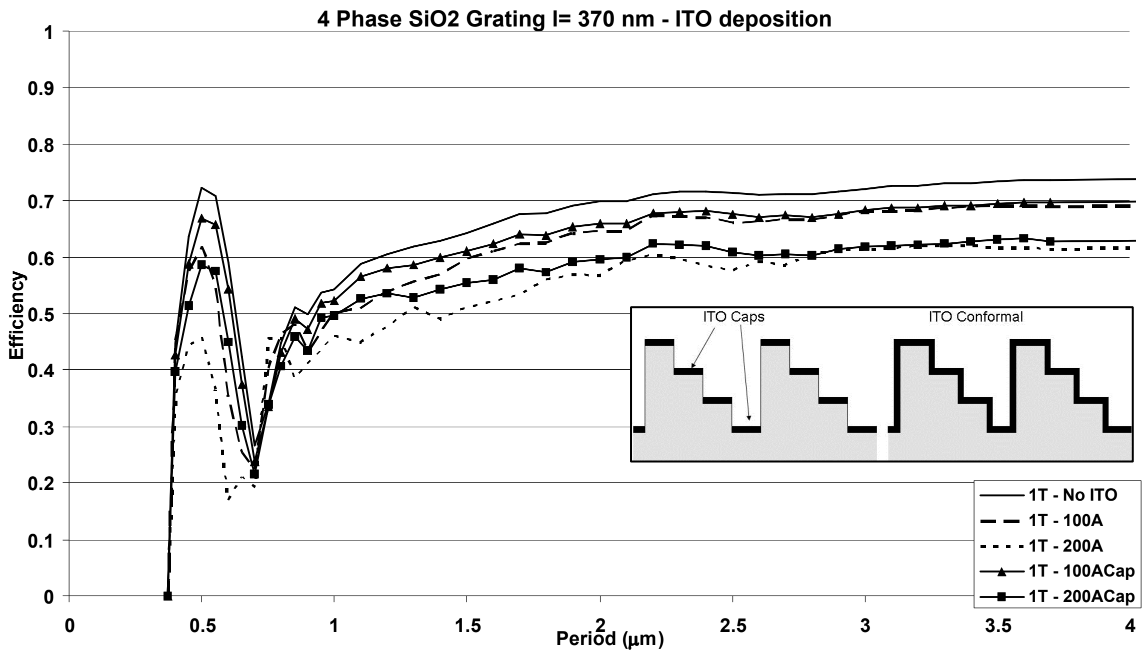

Figure 10 RCWA simulations of the first transmitted order for four-level diffractives as function of the period size for a fixed depth. The simulation uses a wavelength of 0.37µm, a 45-degree polarization, and normal incidence in fused silica with 100Å and 200Å of ITO and no ITO on the DOE.

6. CONCLUSIONS

In this paper, we have described the use of diffractive lenses in large numerical aperture applications. The lenses can be fabricated using well-known semiconductor techniques, allowing for excellent control of aberrations while maintaining a small package.

We showed techniques to improve the efficiency of DOEs, including changing the depth of the gratings and changing their geometry. We also looked at the effects of coating the lenses with a thin film of ITO and how it reduces DOE efficiency as the coating gets thicker.

ACKNOWLEDGMENT

Sandia is a multiprogram laboratory operated by Sandia Corporation, a Lockheed Martin Company, for the United States Department of Energy's National Nuclear Security Administration under contract DE-AC04-94AL85000.

REFERENCES

1. D. J. Wineland, C. Monroe, W. M. Itano, D. Leibfried, B. E. King, and D. M. Meekhof, “Experimental issues in coherent quantum-state manipulation of trapped atomic ions,” *J. Res. NIST* **103**, 259-328, 1998.

2. D. Kielpinski, C. Monroe, and D. J. Wineland, “Architecture for a large-scale ion-trap quantum computer,” Nature **,417**, 709-711, 2002.

3. R. Menon, D. Gil, and H. I. Smith, “Experimental characterization of focusing by high-numerical aperature zone plates,” JOSA A, **23**, 567-571, 2006.

4. B. B. Blinov, D. L. Moehring, L.- M. Duan and C. Monroe, "Observation of entanglement between a single trapped atom and a single photon," Nature **428**, 153–157, 2004.

5. M.G. Moharam, E.B. Grann, D.A. Pommet and T.K. Gaylord, “Formulation for stable and efficient implementation of the rigorous coupled-wave analysis of binary gratings,” JOSA A, **12**, 1068-1076, 1995.

6. G.J. Swanson, “Binary optics technology: theoretical limits on the diffraction efficiency of multilevel diffractive optical elements,” Technical Report 914, Lincoln Laboratory, Massachusetts Institute of Technology, 1991.

7. V. Craciun, D. Craciun, Z. Chen, J. Hwang, R.K. Singh, “Room Temperature Growth Of Indium Tin Oxide Films By Ultraviolet-Assisted Pulsed Laser Deposition,” Mat. Res. Soc. Symp. **617**, J3.13, 2000.